


FULL-LENGTH ORIGINAL RESEARCH

Dynamic tractography-based localization of spike sources and animation of spike propagations

Takumi Mitsuhashi^{1,2} | Masaki Sonoda^{1,3} | Kazuki Sakakura^{1,4} |
Jeong-Won Jeong^{1,5} | Aimee F. Luat^{1,5,6} | Sandeep Sood⁷ | Eishi Asano^{1,5} 

¹Department of Pediatrics, Children's Hospital of Michigan, Detroit Medical Center, Wayne State University, Detroit, Michigan, USA

²Department of Neurosurgery, Juntendo University, Tokyo, Japan

³Department of Neurosurgery, Yokohama City University, Yokohama, Kanagawa, Japan

⁴Department of Neurosurgery, University of Tsukuba, Tsukuba, Japan

⁵Department of Neurology, Children's Hospital of Michigan, Detroit Medical Center, Wayne State University, Detroit, Michigan, USA

⁶Department of Pediatrics, Central Michigan University, Mt. Pleasant, Michigan, USA

⁷Department of Neurosurgery, Children's Hospital of Michigan, Detroit Medical Center, Wayne State University, Detroit, Michigan, USA

Correspondence

Eishi Asano, Division of Pediatric Neurology, Children's Hospital of Michigan, Wayne State University, 3901 Beaubien St., Detroit, MI 48201, USA.
Email: easano@med.wayne.edu

Funding information

Core Research for Evolutional Science and Technology, Grant/Award Number: JPMJCR1784; National Institute of Neurological Disorders and Stroke, Grant/Award Number: NS064033 and NS089659

Abstract

Objective: This study was undertaken to build and validate a novel dynamic tractography-based model for localizing interictal spike sources and visualizing monosynaptic spike propagations through the white matter.

Methods: This cross-sectional study investigated 1900 spike events recorded in 19 patients with drug-resistant temporal lobe epilepsy (TLE) who underwent extraoperative intracranial electroencephalography (iEEG) and resective surgery. Twelve patients had mesial TLE (mTLE) without a magnetic resonance imaging-visible mass lesion. The remaining seven had a mass lesion in the temporal lobe neocortex. We identified the leading and lagging sites, defined as those initially and subsequently (but within ≤ 50 ms) showing spike-related augmentation of broadband iEEG activity. In each patient, we estimated the sources of 100 spike discharges using the latencies at given electrode sites and diffusion-weighted imaging-based streamline length measures. We determined whether the spatial relationship between the estimated spike sources and resection was associated with postoperative seizure outcomes. We generated videos presenting the spatiotemporal change of spike-related fiber activation sites by estimating the propagation velocity using the streamline length and spike latency measures.

Results: The spike propagation velocity from the source was 1.03 mm/ms on average (95% confidence interval = .91–1.15) across 133 tracts noted in the 19 patients. The estimated spike sources in mTLE patients with International League Against Epilepsy Class 1 outcome were more likely to be in the resected area (83.9% vs. 72.3%, $\phi = .137$, $p < .001$) and in the medial temporal lobe region (80.5% vs. 72.5%, $\phi = .090$, $p = .002$) than those associated with the Class ≥ 2 outcomes. The resulting video successfully animated spike propagations, which were confined within the temporal lobe in mTLE but involved extratemporal lobe areas in lesional TLE.

Significance: We have, for the first time, provided dynamic tractography visualizing the spatiotemporal profiles of rapid propagations of interictal spikes

through the white matter. Dynamic tractography has the potential to serve as a unique epilepsy biomarker.

KEYWORDS

diffusion tensor imaging, electrocorticography, epileptic network, interictal epileptiform activity, irritative zone, pediatric epilepsy surgery

1 | INTRODUCTION

The goals of this retrospective study include visualizing monosynaptic propagations of interictal spike discharges through the white matter tracts. The hallmarks of an interictal spike discharge in focal epilepsy include its rapid propagation from a cortical area to others.¹ Previous studies of patients with temporal lobe epilepsy (TLE) using scalp electroencephalography (EEG), magnetoencephalography (MEG), or intracranial EEG (iEEG) have estimated that spike propagation takes place at a velocity of 1.2–3.0 mm in Euclidean distance per millisecond.^{2–4} Nonetheless, the assumption of linear neural propagations may not be biologically plausible. Instead, the underlying white matter tracts are suggested to be the critical pathways that allow monosynaptic neural propagations to remote cortical regions in 50 ms or less.^{3,5} The causal evidence from invasive human studies supports this notion. Disconnection of the white matter tracts eliminated propagations of spike discharges to remote regions.⁶ Electrical stimulation of the irritative zones replicated the propagation pattern of spontaneous spike discharges.⁷ Electrical stimulation of the gray and white matter sites likewise induced neural propagations at areas several centimeters away from the stimulus site within 50 ms.^{8,9} Such rapid neural propagations are difficult to attribute to the intracortical slow horizontal propagation, whose velocity is estimated to range from .006 to .009 cm/ms.^{10,11} Multisynaptic propagations, including those through the corticothalamocortical pathways, are suggested to take at least 70 ms.^{3,5,12} In the present study of monosynaptic spike propagations in patients with drug-resistant TLE, we thus identified the events of interictal spikes that propagated to other regions within 50 ms on iEEG recording and had a supporting white matter tract on diffusion-weighted imaging (DWI) tractography. We built a video animating the spike-related fiber activations from the leading to lagging sites through the white matter tracts, using a method similar to those reported in our previous studies of neural propagations induced by single-pulse electrical stimulation (SPES).^{13,14}

Intracranially recorded spike discharges are suggested to have clinical utility. Previous iEEG studies reported that resection of electrode sites generating spikes frequently or those preceding others was predictive of successful seizure

Key Points

- Dynamic tractography, for the first time, has animated spike propagations through the white matter tracts in temporal lobe epilepsy
- The novel model incorporating the white matter length from intracranial electrode sites estimated the sources of spike discharges
- Resection of the regions, including the estimated spike sources, was associated with post-operative seizure control

control.^{15–17} However, one cannot completely rule out the possibility that the true spike generator may have been unsampled by intracranial electrodes.^{18,19} In the present study, we estimated the source/origin of spike discharges using the tractography-based streamline length of white matter tracts from intracranial electrode sites and observed spike latencies at given sites. We built a video animating the spike propagating from the estimated source through the white matter. We validated our source localization method by testing the hypothesis that a higher proportion of spike sources would be included in the resection in patients with International League Against Epilepsy (ILAE) Class 1 outcome than those failing to achieve such success.

As an ancillary analysis for patients with a magnetic resonance imaging (MRI)-visible mass lesion, we generated another video showing the spike propagations from the perilesional cortical site. Previous iEEG studies have reported that interictal spikes or ictal discharges may originate from not the lesion but the cortex adjacent to or overlying a structural lesion.^{20–23}

2 | MATERIALS AND METHODS

2.1 | Participants

The inclusion criteria consisted of extraoperative iEEG monitoring at Children's Hospital of Michigan in Detroit between September 2007 and August 2019, age at surgery was 4 years and older,²⁴ and diagnosis of ipsilateral TLE was confirmed by the iEEG-based seizure onset zone

(SOZ).¹⁵ The exclusion criteria included multifocal mass lesions on MRI, malignant tumor suspected on MRI, history of previous resective surgery,²⁵ and postoperative follow-up shorter than 1 year.²⁶ We studied all patients who satisfied the eligibility criteria (Figure S1). The institutional review board at Wayne State University has approved the present study. We obtained informed consent from the legal guardians of patients and assent from pediatric patients.

2.2 | Intracranial electrode placement and extraoperative iEEG recording

Following the Phase 1 evaluation, we placed platinum subdural electrodes (10-mm center-to-center distance) on the pial surface of the hemisphere suspected to be responsible for habitual seizures (Figure 1). The spatial extent of extraoperative iEEG sampling was determined based on the clinical need.^{15,25} Strip electrodes sampled iEEG signals from the mesial temporal lobe structures, including the hippocampal, parahippocampal, entorhinal, and amygdala regions. Grid electrodes covered the lateral temporal and extratemporal lobe regions.

To determine the boundary between the SOZ and eloquent areas, we performed extraoperative video-iEEG recording for 2–7 days, as previously reported.²⁵ The sampling rate was 1000 Hz, and the amplifier bandpass was .016–300 Hz. We excluded artifactual channels from further analysis. All quantitative iEEG analysis was performed using common average reference.

2.3 | Magnetic resonance imaging

Before the intracranial electrode placement, we acquired 3-T MRI, including T1-weighted spoiled gradient-recalled echo and fluid-attenuated inversion recovery sequences.²⁵ For each patient with an MRI-visible mass lesion, board-certified neurosurgeons T.M. and K.S. localized the perilesional cortical site, the cortex most proximal to the center of the lesion. We generated a three-dimensional surface image with implanted subdural electrodes displayed on the pial surface.^{25,27–29} The FreeSurfer script (<http://surfer.nmr.mgh.harvard.edu>) spatially normalized given electrode sites to the standard Montreal Neurological Institute (MNI) space (Figure 1).^{14,25}

2.4 | Patient profile and classification

Table 1 shows the patient profile. Figure S1 shows the participant flow diagram. We classified patients into those with or without an MRI-visible mass lesion and intended to generate the dynamic tractography videos for each patient group. Seven patients had an MRI-visible mass lesion outside the hippocampus; thus, they were treated as lesional TLE patients. All lesional patients achieved ILAE Class 1 outcome following surgical resection. The remaining 12 patients without a mass lesion had the SOZ at the mesial temporal lobe region; thus, they were treated as mesial TLE (mTLE) patients. Eight mTLE patients achieved ILAE Class 1 outcome after surgery, whereas the remaining four failed. The mean postoperative follow-up period was 28.7 months (SD = 13, range = 12–64). All study patients had complete resection of the SOZ. We

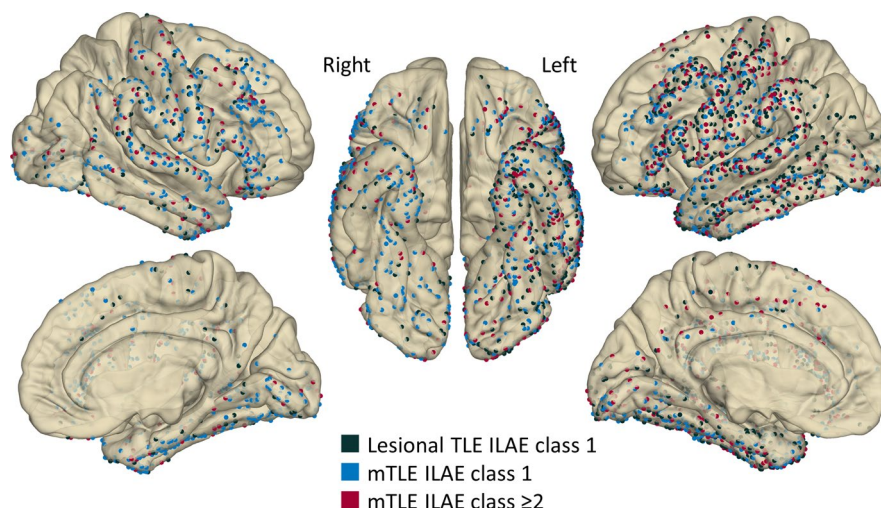


FIGURE 1 The anatomical locations of intracranial electrode contacts included in the analysis. Dark green represents seven patients with lesional temporal lobe epilepsy (TLE), all of whom achieved International League Against Epilepsy (ILAE) Class 1 outcome after resective surgery. Light blue represents eight patients with mesial TLE (mTLE) who had Class 1 outcome. Red represents four patients with mTLE who failed to achieve Class 1 outcome (Class 2, $n = 1$; Class 3, $n = 3$)

TABLE 1 Patient profile

Characteristic	Value
Total patients, <i>N</i>	19
Mean age, years (range)	12.8 (5–17)
Male patients, <i>n</i> (%)	10 (52.6)
Left-hemispheric epilepsy, <i>n</i> (%)	13 (68.4)
Mean number of antiepileptic drugs	1.9
MRI findings, <i>n</i> (%)	
Tumor	6 (31.6)
Dysplasia	1 (5.2)
No mass lesion	12 (63.2)
Pathology in patients with no MRI-visible mass lesion, <i>n</i> (%)	
Gliosis + hippocampal neuronal loss ^a	8 (42.1)
Gliosis alone	2 (10.5)
Gliosis + hippocampal neuronal loss + dysplasia ^a	1 (5.2)
Gliosis + dysplasia	1 (5.2)

Abbreviation: MRI, magnetic resonance imaging.

^aNine patients showed pathological findings consistent with a diagnosis of hippocampal sclerosis.

analyzed 100.6 (SD = 22.1) electrodes per patient on average (Figure 1). None of the study patients had missing iEEG or MRI data.

2.5 | Visual identification and quantitative analysis of interictal spikes

We initially defined a spike discharge as a sharply contoured wave, which was immediately followed by a slow wave, clearly distinguished from the background activity and unattributable to an amplitude fluctuation of the background rhythm.^{1,30} In each patient, we visually identified 100 representative spike events, which occurred during an artifact-free non-rapid eye movement sleep period, at least 2 h apart from ictal events, and at least 1.5 s apart from other interictal spike events.^{25,31}

We employed the following three-step procedure to localize the leading site showing interictal spike-related broadband augmentation earliest among all electrode sites. Step 1 was marking each of the 100 visually largest spikes. For each of the 100 visually identified spike events, we visually marked the peak of the largest negative deflection among all channels. Step 2 was quantitative identification of the site showing the largest spike. We performed Morlet wavelet time–frequency analysis using the FieldTrip toolbox (<http://www.fieldtriptoolbox.org/>). We transformed iEEG voltage signals during

a 2000-ms period centered on each visual spike marking into time–frequency bins at a 20–70 Hz broadband range (2-Hz frequency bins; a given frequency band was divided by seven cycles, sliding in 1-ms steps).^{14,32} We computed the percent change of broadband amplitude augmentation at each channel compared to that during the 300-ms baseline period (–1000 to –700 ms before the marking). We then determined the largest spike channel, defined as the electrode site showing the highest spike-related broadband amplitude augmentation (taking place within 50 ms before or after the visual marking) on average across 100 spike events visually identified in each patient. Step 3 was quantitative localization of the leading and lagging sites. We performed the final time–frequency analysis on the 2000-ms period centered on the peak of broadband augmentation at the largest spike channel defined in Step 2 mentioned above; this peak time was treated as the 0-ms point in this analysis. We likewise used the percent change of spike-related broadband amplitude augmentation for Step 3 analysis. The cluster-based permutation test determined whether a given channel showed a significantly reproducible amplitude augmentation (cluster randomization = 200, cluster size threshold $\alpha = .05$).³³ We then *z*-score transformed the individual spike-related broadband amplitudes relative to that during the 300-ms baseline period mentioned above. We defined a significant spike as broadband amplitude augmentation with a *z*-score > 10 taking place within 50 ms before or after the 0-ms point (Figure S2).³⁴ The spike latency was defined as the moment when the *z*-score reached 10 at a given site. The leading site was defined as that with the mean spike latency earliest among all sites. The lagging sites were defined as the remaining sites showing a *z*-score > 10 in at least 5% of the 100 analyzed spike events.

2.6 | Anatomical tractography to localize white matter tracts connecting cortical sites

As previously performed,^{14,35} we generated DWI tractography using the open-source data averaged across the 1065 individuals participating in the Human Connectome Project (<http://brain.labsolver.org/diffusion-mri-templates/hcp-842-hcp-1021>).³⁶ We validated our analytic approach by demonstrating that the spatial patterns of SPES-induced neural propagations based on the open-source DWI data were similar to those based on the individual data.³⁵

We placed seed-spheres of a radius of 4 mm at leading, lagging, and perilesional cortical sites. Within the

MNI space, DSI Studio (<http://dsi-studio.labsolver.org/>) generated streamlines between the leading and lagging sites in all 19 patients. We likewise generated streamlines between the perilesional and leading/lagging cortical sites in seven lesional patients. We considered streamlines satisfying the following criteria to be significant and present: a fractional anisotropy threshold of .3, a maximum turning angle of 70°, step size of .3 mm, and streamline length from 10 to 250 mm. As previously performed,¹⁴ we included the shortest significant streamline connecting each seed region pair in the following analyses.

2.7 | Tractography-based source localization of interictal spike discharges

For each of the 100 spike events of each patient, we estimated the spike source/origin to plausibly induce monosynaptic propagations at lagging sites at given observed latencies. We placed up to 1000 candidate streamlines of a length of ($V_{\text{Proxy}} \times [T_{\text{Before}} + T_{\text{Spike}}]$) mm from each leading/lagging site (Figure 2A,B); thereby, the tip of each streamline had a "candidate source sphere" of a radius of 4 mm. The V_{Proxy} was the proxy spike propagation velocity, defined as (the streamline length between the leading and lagging sites) divided by (the observed latency at given lagging sites), averaged across all seven lesional cases. The T_{Spike} was treated as 0 (ms) at the leading site and the observed latency at a given lagging site. The source was presumed to generate a spike discharge T_{Before} (ms) before the leading site did. We determined which of the following 25 candidate odd numbers below 50 (i.e., 1, 3, ..., and 49 ms) would be the best-fit T_{Before} , which resulted in the densest distribution of candidate source spheres at a focal cortical area (as reflected by the minimum entropy of the sphere distribution; Figure 2C). Thereby, the center of gravity of the distributed spheres was treated as the source/origin of a given spike discharge (Figure 2D).

2.8 | Association between spike latency and streamline length

A mixed model analysis tested the hypothesis that delayed spike latency at a lagging site would be associated with a longer streamline length from the leading and perilesional cortical sites. The dependent variable was the streamline length on tractography. The fixed effect predictor variable was the spike latency. The random factors included patients and intercept.

2.9 | Association between spike source removal and postoperative seizure outcome in mTLE patients

We tested the hypothesis that 800 spike events seen in mTLE patients with ILAE Class 1 outcome would have a higher proportion of candidate source spheres within the resected area than 400 spike events of those failing to have such outcome (Mann-Whitney *U*-test). Likewise, the chi-squared test determined whether the spike sources were more likely to be in the resected area in ILAE Class 1 than Class ≥ 2 . Finally, the *t*-test compared the resection volume between the two groups; the extent of surgical resection was measured based on the intraoperative photographs taken immediately before dural closure; we validated this analytic approach previously using the data from 89 patients.²⁵

2.10 | Visualization of spike propagations

We have generated three types of dynamic tractography videos visualizing propagations of spike discharge (averaged across 100 events) through the white matter tracts using a method similar to that reported previously.¹⁴ Each video visualizes the spatiotemporal changes of spike-induced fiber activation sites along the streamlines with a temporal resolution of 1 ms. In Videos S1A and S2A, the model assumes that the leading site was the generator. We have visualized spike propagations from the leading to lagging sites; thereby, the propagation velocity was defined as (the streamline length) divided by (T_{Spike}). In Videos S1B and S2B, the model assumes that the estimated source was the generator. We have visualized spike propagations from the source to both leading and lagging sites. The propagation velocity was assumed to be V_{Proxy} between the source and leading site and (the streamline length) divided by ($T_{\text{Before}} + T_{\text{Spike}}$) between the source and a given lagging site. In Video S2C, the model assumes that the perilesional cortical site was the generator. The propagation velocity between the perilesional and leading site was defined as (V_{Proxy}) and (the streamline length) divided by ($T_{\text{Before}} + T_{\text{Spike}}$) between the perilesional and a given lagging site.

We have created a video visualizing the dynamics of cortical modulations related to spike discharges (averaged across 100 events) seen in each group of mTLE patients (Video S3). The video delineated the spatiotemporal changes in broadband amplitude at leading and lagging sites with a temporal resolution of 1 ms using a method similar to that previously reported.³⁷

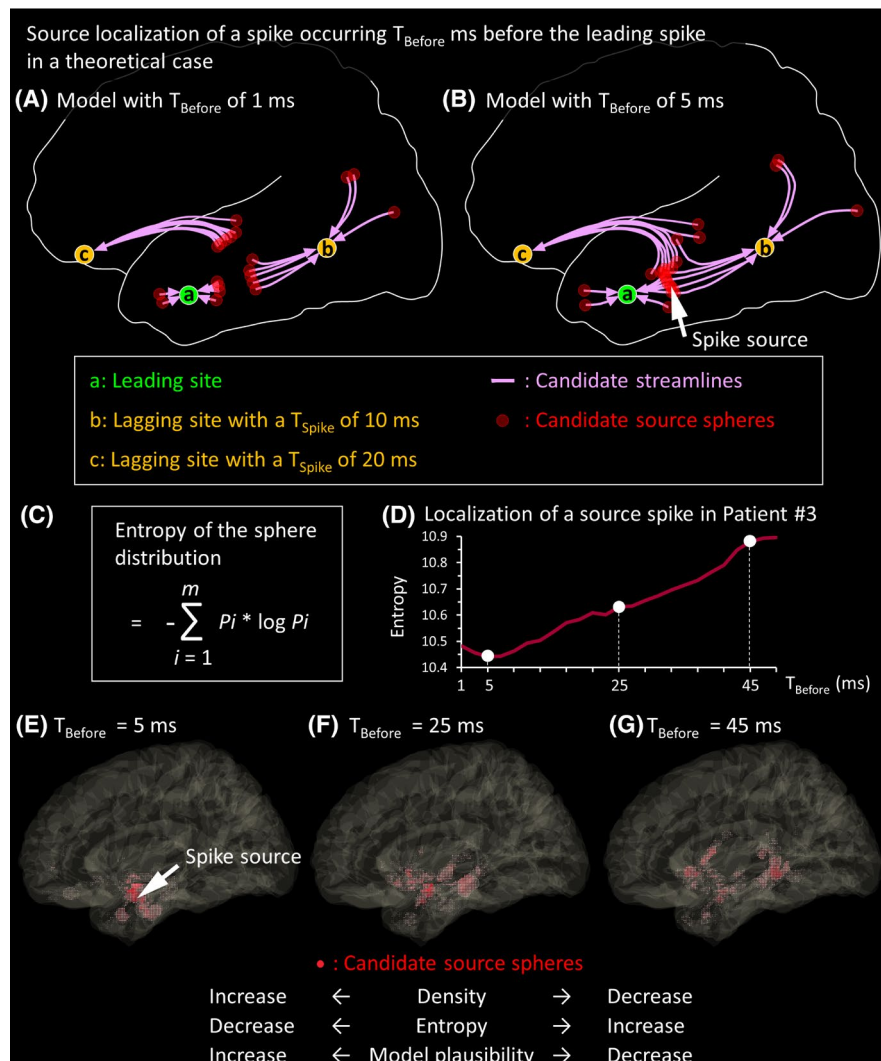


FIGURE 2 Tractography-based source localization of interictal spikes. (A, B) The schematic illustrations present the concept of our tractography-based source localization in a scenario where Channel a is the leading site, Channel b is a lagging site with a spike latency (T_{Spike}) of 10 ms, and Channel c is a lagging site with a T_{Spike} of 20 ms. (A) The model with T_{Before} of 1 ms results in a scarce spatial distribution of candidate source spheres; thus, none of the resulting spheres plausibly induces spike propagations at these lagging sites at the given observed latencies. (B) The model with T_{Before} of 5 ms results in the densest distribution of candidate source spheres; the spike source will comprise the center of gravity of spheres (arrow). The source is estimated to be located where the spike would occur 5 ms before the leading site. This model indicates that the spike would propagate from the source to the leading site in 5 ms. (C) The formula to compute the entropy of the sphere distribution is presented. Thereby, m is the total number of 1-mm voxels comprising the entire space occupied by all spheres delineated with a given T_{Before} . P_i is (the number of candidate source spheres directly affecting the i -th voxel) divided by (the total number of voxels included in all spheres). (D–G) The empirical data from a spike event observed in Patient #3 are presented. (D) The relationship between the T_{Before} and the entropy of sphere distribution is shown. (E) T_{Before} of 5 ms achieved the minimum entropy of the sphere distribution; in other words, the densest distribution of spheres (red shaded areas) was achieved at a focal area. The arrow denotes the estimated source of this spike discharge. Because the V_{Proxy} was found to be 1.46 ms in the present study, the spike source was suggested to be 7.3 mm (i.e., 1.46×5) away from the leading site. (F, G) T_{Before} of 25 ms (F) or 45 ms (G) failed to achieve a unifocal distribution of spheres; thus, we considered these latencies less plausible than 5 ms for localizing the spike source

2.11 | Statistical analysis

Statistical analyses were performed using SPSS Statistics Version 27 (IBM) and Statistical and Machine Learning Toolbox MATLAB 2018b (MathWorks). The significance was set at a p -value of .05.

2.12 | Data and code availability

All iEEG data, as well as the MATLAB-based codes for the dynamic tractography and tractography-based source localization, are available upon request to the corresponding author.

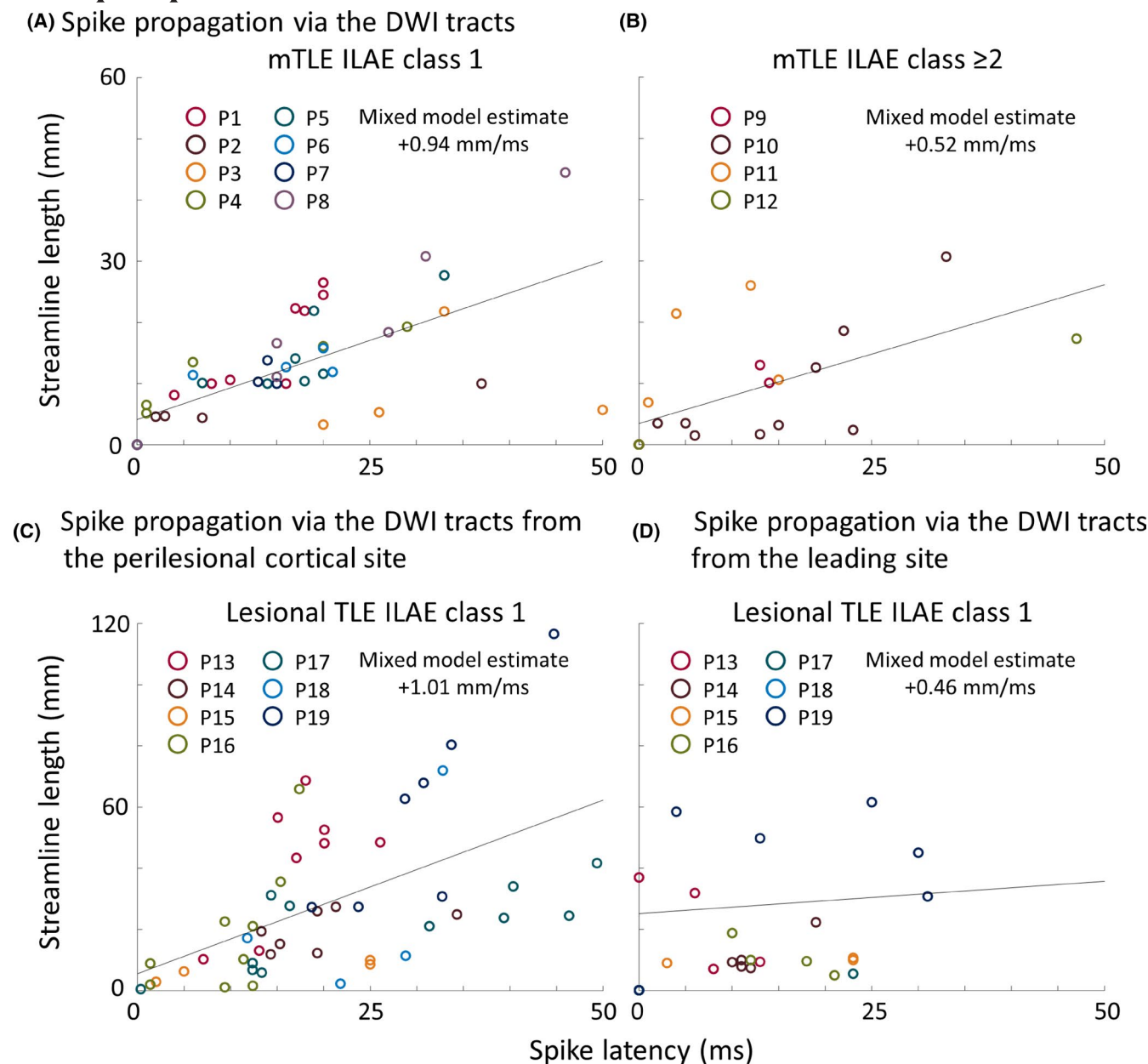


FIGURE 3 Association between the spike latency and tractography-based streamline length. (A, B) The scatter plots derived from mesial temporal lobe epilepsy (mTLE) patients. Each circle reflects the relationship between the spike latency and streamline length from the leading site in mTLE patients with International League Against Epilepsy (ILAE) Class 1 (A) and Class ≥ 2 (B). (C, D) The scatter plots derived from lesional TLE patients. Each circle reflects the relationship between the spike latency and streamline length from the perilesional cortical site (C) and from the leading site (D). Circle color reflects a given patient. Dotted line: regression line. DWI, diffusion-weighted imaging

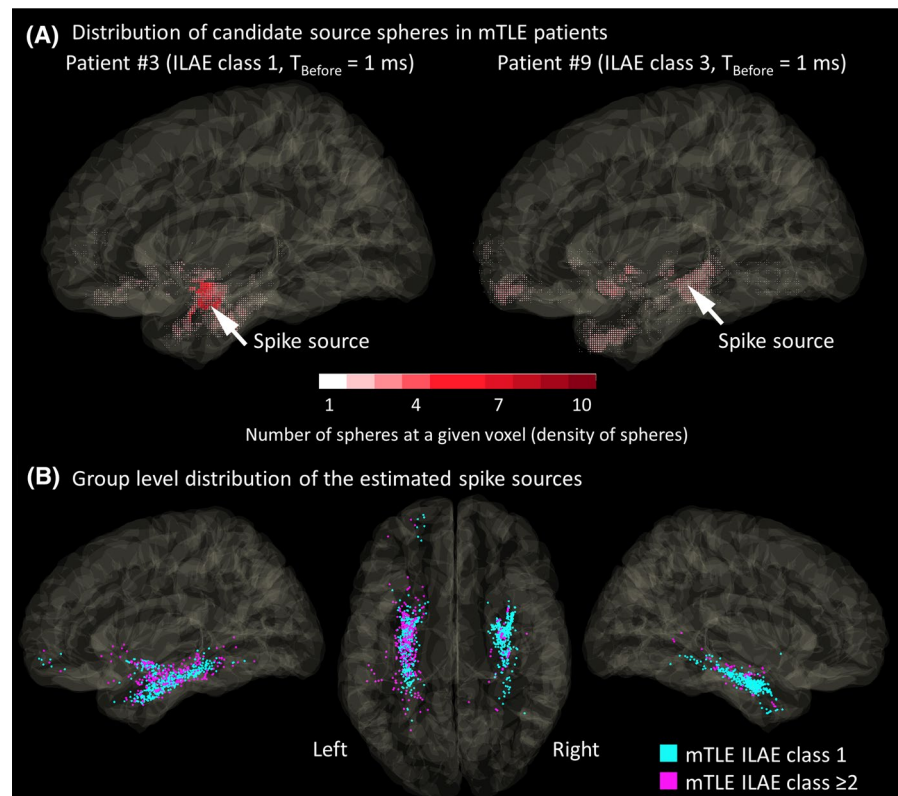
3 | RESULTS

3.1 | Association between spike latency and tractography-based streamline length

Lagging sites with delayed spike latency had longer streamlines from the leading site in mTLE ILAE Class 1 (mixed model estimate = +.94 mm/ms, $t = +6.105$, $p < .001$; Figure 3A) and Class ≥ 2 (mixed model

estimate = +.52 mm/ms, $t = +3.901$, $p = .001$; Figure 3B). Likewise, delayed spike latency was associated with longer streamlines from the perilesional cortical site in lesional TLE (mixed model estimate = +1.01 mm/ms, $t = +4.290$, $p < .001$; Figure 3C). Such a positive correlation between spike latency and streamline length from the leading site was not replicated in lesional TLE (mixed model estimate = +.46 mm/ms, $t = +1.699$, $p = .102$; Figure 3D).

FIGURE 4 The distribution of spike sources. (A) The distributions of candidate source spheres for a spike event of Patients #3 and #9. Each dot indicates the location of a candidate source sphere. The dot color reflects the density of candidate source spheres at a given voxel. For each spike event, the spike source (arrow) was defined to be localized at the center of gravity of these spheres. (B) Distribution of spike sources seen in 12 patients with mesial temporal lobe epilepsy (mTLE). Cyan dots indicate 800 spike sources seen in patients with the International League Against Epilepsy (ILAE) Class 1 outcome. Magenta dots indicate 400 spike sources in those with Class ≥ 2 outcomes



3.2 | Distribution of candidate source spheres in mTLE patients

Figure 4A shows representative distributions of candidate source spheres of spikes seen in two different patients. In Patient #3 (mTLE ILAE Class 1), the sphere distribution was clustered in the anterior medial temporal lobe. In Patient #9 (Class ≥ 2), the sphere distribution was sparse and involved the posterior temporal and frontal lobes. Group-level analysis of 1200 spike events of mTLE patients revealed that the events in the Class 1 patients had a higher proportion of candidate source spheres included within the resected area than those in Class ≥ 2 (median = 38.4% vs. 28.6%, $p < .001$, Mann-Whitney U -test; Figure S4A). Likewise, spike events in the Class 1 patients had a higher proportion of candidate source spheres within the temporal lobe cortex than those in Class ≥ 2 (median = 79.5% vs. 66.0%, $p < .001$; Figure S4C). The resection volume was not different between the two outcome groups (Class 1: 52.6 cm³ [95% confidence interval (CI) = 32.4–72.9] vs. Class ≥ 2 : 55.9 cm³ [95% CI = 26.5–85.2], $p = .805$, t -test; Figure S4B).

3.3 | Relationship between resection of estimated spike sources and postoperative seizure outcome in mTLE patients

A substantial proportion of the spike sources were localized in the hippocampus (26.4% in Class 1 and

20.6% in Class ≥ 2), amygdala (8.9% and 17.6%), and parahippocampal–entorhinal gyrus (45.3% and 34.5%). In mTLE ILAE Class 1 compared to Class ≥ 2 , the estimated spike sources were more likely to be in the resected area (83.9% vs. 72.3%, $\phi = .137$, $p < .001$, chi-squared test) and in the medial temporal lobe region (80.5% vs. 72.5%, $\phi = .090$, $p = .002$; Figure 4B). The Euclidean distance between the estimated spike sources and the leading site was shorter in mTLE ILAE Class 1 than Class ≥ 2 (12.9 mm vs. 23.7 mm, $p < .001$, Mann-Whitney U -test).

3.4 | Dynamic tractography-based visualization of spike propagations in mTLE

The dynamic tractography successfully animated the rapid spike propagations through 40 white matter streamlines from the leading site in eight mTLE Class 1 patients (Video S1A; Figure 5). Spikes propagated in a posterior-to-anterior direction in 47.5% (19/40) and in the opposite direction in 52.5% (21/40). All streamlines ended within the temporal lobe (Video S1A). Likewise, the spike-related cortical modulations were restricted to the temporal lobe (Video S3). The mean streamline length was 14.5 mm (95% CI = 11.8–17.1).

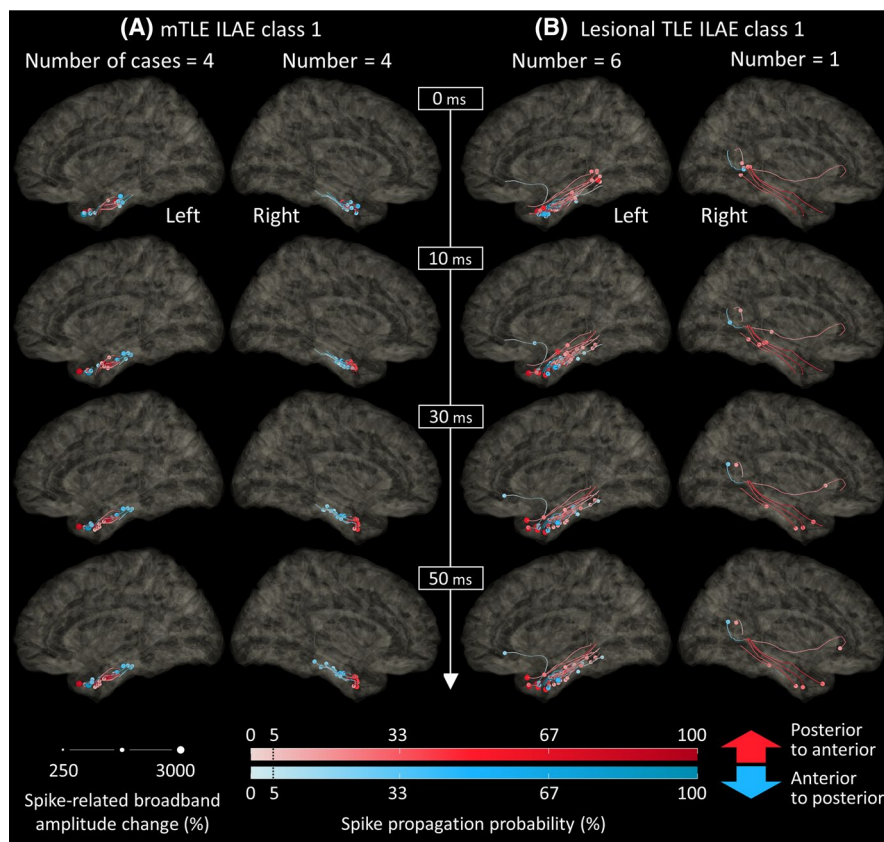


FIGURE 5 Snapshots of dynamic tractography. The dynamic tractography, derived from the intracranial electroencephalography and diffusion-weighted imaging data, animates the monosynaptic spike propagations through the white matter tracts. (A) The snapshots of spike propagations in eight mesial temporal lobe epilepsy (mTLE) patients who achieved International League Against Epilepsy (ILAE) Class 1 outcome; 0 ms reflects the spike onset at the leading site (Video S1A). Circles denote spike propagation-related fiber activation sites at a given moment. Circle size reflects spike-related broadband amplitude change (%) measured at a given lagging site. Color density represents spike propagation probability (%) calculated at a given lagging site. Red indicates propagation in a posterior-to-anterior direction. Blue indicates propagation in an anterior-to-posterior direction. (B) Spike propagations in seven lesional TLE patients, all of whom achieved ILAE Class 1 outcome; 0 ms reflects estimated spike onset at the perilesional cortical site

3.5 | Dynamic tractography-based visualization of spike propagations in lesional TLE

We animated the spike propagations through 49 streamlines from the perilesional cortical site in seven lesional TLE Class 1 patients (Video S2C). Spikes propagated in a posterior-to-anterior direction in 65.3% (32/49) and the opposite direction in 34.7% (17/49; Figure S3). In lesional TLE, 91.8% (45/49) ended within the temporal lobe, 4.1% (2/49) in the frontal lobe, and 4.1% (2/49) in the parietal lobe. The mean streamline length was 27.5 mm (95% CI = 20.5–34.5). The model assuming spike propagations from the leading site indicated that the propagation velocity was highly variable across the streamlines (Video S2A), as predicted by the results of the mixed model failing to

show a positive correlation between the spike latency and streamline length (Figure 3D).

3.6 | Dynamic tractography-based visualization of spike propagations from estimated source

The dynamic tractography successfully animated rapid spike propagations from the source to leading/lagging sites; the mean spike propagation velocity was 1.03 mm/ms (95% CI = .91–1.15) across 133 tracts noted in the 19 patients. The Euclidean distance between the source and the center of the lesion was 23.9 mm on average across seven lesional patients (95% CI = 8.9–38.9).

4 | DISCUSSION

4.1 | Significance and innovation of dynamic tractography

To our best knowledge, this is the first-ever study that animates the spatiotemporal dynamics of spike propagations through the white matter tracts in patients with focal epilepsy. The dynamic tractography successfully visualized the networks of interictal spike discharges and characterized the directions of their propagations. Thus, the resulting videos may be helpful for patients and neuroscience students to understand the mechanism and process of focal epilepsy. For example, in our mTLE patients, spikes propagated in a posterior-to-anterior direction in 47.5% and the opposite direction in 52.5%. Studies of healthy nonhuman primates have demonstrated the posterior-to-anterior fiber projections in the medial temporal lobe structures.³⁸ In contrast, previous studies of mTLE patients using scalp EEG and MEG estimated that interictal spike discharges would propagate in an anterior-to-posterior direction.^{39,40} Investigators have emphasized that understanding the epileptic networks, including the directions of propagations of epileptiform discharges, would be crucial for planning a disconnective surgery to prevent a clinical seizure and protect healthy brain tissues.⁴¹ Some reported excellent seizure control after disconnecting the epileptogenic zone from the symptomatogenic and eloquent cortices.⁴²

We provided internal and external validity to our dynamic tractography for visualizing spike propagations in mTLE. We found that the spike latency at lagging sites was linearly and positively correlated to the length of streamline from the leading site in mTLE. All of the monosynaptic spike propagations observed in our mTLE patients were restricted within the temporal lobe (Video S1). In contrast, lesional TLE patients had subsets of spike propagations involving the extratemporal lobe structures (Video S2). These observations are consistent with the results of a previous scalp EEG study of 30 patients with drug-resistant TLE.⁴³ mTLE patients without dual pathology had a higher probability of interictal spikes localized in the anterior temporal lobe region than those with temporal lobe tumors (95.2% vs. 0%).⁴³

We built and validated a novel source localization method. The innovation lies in incorporating the length of white matter tracts allowing monosynaptic spike propagations. We found that the spike sources in mTLE patients with ILAE Class 1 outcome were more likely to be in the resected area (83.9% vs. 72.3%) and the medial temporal lobe region (80.5% vs. 72.5%) than those failing to achieve such success. The Euclidean distance between the estimated spike sources and the leading site was

shorter in mTLE ILAE Class 1 than Class ≥ 2 (12.9 mm vs. 23.7 mm). The spike propagation velocity from the source was 1.03 mm/ms on average across 133 tracts noted in the 19 patients. We believe that this observed velocity is consistent with the ones previously estimated with different modalities, considering that spikes do not propagate in a straight line but through the curving white matter tracts. Previous iEEG studies of TLE patients reported that the spike propagation velocity would range from 1.2 to 3.0 mm (Euclidean distance) per millisecond.^{3,4} A study of mTLE patients using scalp EEG and MEG estimated the spike propagation from the deep to superficial temporal cortices would occur with a velocity of 1.2–2.9 mm/ms.² Nonetheless, these noninvasive modalities have limitations in the spatial accuracy of source localization in deep brain regions, including the medial and basal temporal lobes.^{44,45}

Extensive prospective studies should clarify the utility of the tractography-based spike source localization in presurgical evaluation. For example, we still do not know how many spike sources should be removed to optimize the postoperative seizure outcome. Figure S5 shows the results of an ancillary receiver operating characteristics analysis performed in the mTLE patients. All six patients with $\geq 80\%$ of the spike sources removed successfully achieved ILAE Class 1 outcome, whereas only two of the six patients with $<80\%$ removed had such surgical success. Investigators may also want to test the hypothesis that tractography is capable of predicting the location and timing of propagation of epileptiform discharges. In Figures S6 and S7, we have provided the preliminary data supporting this hypothesis.

4.2 | Plausible origin of spike generators in lesional TLE

Our study provided observations consistent with the notion that the spike generators may be proximal to the perilesional cortical site in lesional TLE. The model assuming spike propagations from the perilesional cortical site achieved a significant positive correlation between the streamline length and spike latency at a given electrode site (Figure 3C). In contrast, the model assuming spike propagations from the leading site did not show a significant positive correlation between the streamline length and spike latency (Figure 3D). We found that the spike source was localized within 23.8 mm on average from the perilesional cortical site. Based on the results of a meta-analysis of patients with tumor-related focal epilepsy, investigators have advocated more extensive resection than gross total lesionectomy alone to secure postoperative seizure control.²²

4.3 | Methodological considerations

Spatial sampling is an inevitable limitation in any invasive studies. Because subdural electrodes were used to tailor the resection margin, mesial temporal iEEG signals were sampled not from the hippocampal body but mainly from the parahippocampal–entorhinal cortices. Previous studies have suggested that the epileptogenic zone includes the parahippocampal–entorhinal cortices in mTLE; thus, many surgeons resect these mesial temporal lobe structures for optimal seizure control.^{46,47}

We utilized open-source DWI data collected from healthy participants as a part of the human connectome project.³⁶ One may consider that the streamlines generated based on the open-source data are different from those of an individual patient. Partly because of that, we cannot rule out the possibility of false-negative detection of streamlines to some electrode sites receiving a mono-synaptic propagation. Studies have inferred that DWI measures may be altered in the white matter regions proximal to the seizure focus in TLE patients.⁴⁸ Our study patients are children with age ranging from five to 17 years, but white matter myelination continues throughout adolescence and adulthood.⁴⁹ Nonetheless, we have recently demonstrated that the velocity of SPES-induced neural propagations was highly comparable between the open-source and individual DWI data.³⁵

One should consider the effect of volume conduction when electrode sites >10 mm apart exhibit an identical waveform without a time delay.⁵⁰ Based on the visual assessment, we believe that the unwanted effect of volume conduction on our iEEG analysis was small. Electrode sites appeared to record spike discharges generated by the underlying local cortical structure, as reflected by different peak latencies (Figure S8).

The synaptic delay after a given site receives a propagation-related fiber activation has been estimated to range from .5 to 1.1 ms.^{51,52} If the propagation velocity is defined as (the streamline length) divided by ($T_{\text{Spike}} - 1$), the mean velocity from the leading to lagging sites would be computed as 1.17 ms/mm in eight mTLE patients with ILAE Class 1 outcome.

We plan to develop the whole brain-level dynamic tractography atlas incorporating the iEEG data from a large cohort of patients with focal epilepsy in the future. We expect that such a dynamic atlas will visualize the spatiotemporal dynamics of spike propagations common in each type of epilepsy. Our ultimate goals include localizing the potential therapy target and informing clinicians about the concordance between the spike propagation pattern of an individual patient and the typical pattern for a given epilepsy type.

ACKNOWLEDGMENTS

We are grateful to Karin Halsey, BS, REEGT, and Jamie MacDougall, RN, BSN, CPN at Children's Hospital of Michigan for collaboration and assistance in performing the studies described above. This work was supported by the National Institutes of Health (NS064033 to E.A.; NS089659 to J.W.J.) and Japan Science and Technology Agency CREST (JPMJCR1784 to T.M.).

CONFLICT OF INTEREST

None of the authors has any conflict of interest to disclose. We confirm that we have read the Journal's position on issues involved in ethical publication and affirm that this report is consistent with those guidelines.

ORCID

Eishi Asano  <https://orcid.org/0000-0001-8391-4067>

REFERENCES

1. Kural MA, Duez L, Sejer Hansen V, Larsson PG, Rampp S, Schulz R, et al. Criteria for defining interictal epileptiform discharges in EEG. *Neurology*. 2020;94(20):e2139–47.
2. Sutherling WW, Barth DS. Neocortical propagation in temporal lobe spike foci on magnetoencephalography and electroencephalography. *Ann Neurol*. 1989;25(4):373–81.
3. Alarcon G, Guy CN, Binnie CD, Walker SR, Elwes RD, Polkey CE. Intracerebral propagation of interictal activity in partial epilepsy: implications for source localization. *J Neurol Neurosurg Psychiatry*. 1994;57(4):435–49.
4. Fabó D, Maglóczy Z, Wittner L, Pék Á, Erőss L, Czirkák S, et al. Properties of in vivo interictal spike generation in the human subiculum. *Brain*. 2008;131(2):485–99.
5. Matsumoto R, Kunieda T, Nair D. Single pulse electrical stimulation to probe functional and pathological connectivity in epilepsy. *Seizure*. 2017;44:27–36.
6. Ono T, Baba H, Toda K, Ono K. Callosotomy and subsequent surgery for children with refractory epilepsy. *Epilepsy Res*. 2011;93(2–3):185–91.
7. Nayak D, Valentin A, Selway RP, Alarcon G. Can single pulse electrical stimulation provoke responses similar to spontaneous interictal epileptiform discharges? *Clin Neurophysiol*. 2014;125(7):1306–11.
8. Yamao Y, Matsumoto R, Kunieda T, Arakawa Y, Kobayashi K, Usami K, et al. Intraoperative dorsal language network mapping by using single-pulse electrical stimulation. *Hum Brain Mapp*. 2014;35(9):4345–61.
9. Mitsuhashi T, Sonoda M, Iwaki H, Luat AF, Sood S, Asano E. Effects of depth electrode montage and single-pulse electrical stimulation sites on neuronal responses and effective connectivity. *Clin Neurophysiol*. 2020;131(12):2781–92.
10. Chervin RD, Pierce PA, Connors BW. Periodicity and directionality in the propagation of epileptiform discharges across neocortex. *J Neurophysiol*. 1988;60(5):1695–713.
11. Wadman WJ, Gutnick MJ. Non-uniform propagation of epileptiform discharge in brain slices of rat neocortex. *Neuroscience*. 1993;52(2):255–62.

12. van 't Klooster MA, Zijlmans M, Leijten FSS, Ferrier CH, van Putten MJAM, Huiskamp GJM. Time-frequency analysis of single pulse electrical stimulation to assist delineation of epileptogenic cortex. *Brain*. 2011;134(10):2855–66.
13. Silverstein BH, Asano E, Sugiura A, Sonoda M, Lee MH, Jeong JW. Dynamic tractography: integrating cortico-cortical evoked potentials and diffusion imaging. *Neuroimage*. 2020;215:116763.
14. Mitsuhashi T, Sonoda M, Jeong JW, Silverstein BH, Iwaki H, Luat AF, et al. Four-dimensional tractography animates propagations of neural activation via distinct interhemispheric pathways. *Clin Neurophysiol*. 2021;132(2):520–9.
15. Asano E, Juhász C, Shah A, Sood S, Chugani HT. Role of subdural electrocorticography in prediction of long-term seizure outcome in epilepsy surgery. *Brain*. 2009;132(4):1038–47.
16. Klimes P, Cimbalnik J, Brazdil M, Hall J, Dubeau F, Gotman J, et al. NREM sleep is the state of vigilance that best identifies the epileptogenic zone in the interictal electroencephalogram. *Epilepsia*. 2019;60(12):2404–15.
17. Azeem A, von Ellenrieder N, Hall J, Dubeau F, Frauscher B, Gotman J. Interictal spike networks predict surgical outcome in patients with drug-resistant focal epilepsy. *Ann Clin Transl Neurol*. 2021;8(6):1212–23.
18. Schiller Y, Cascino GD, Sharbrough FW. Chronic intracranial EEG monitoring for localizing the epileptogenic zone: an electroclinical correlation. *Epilepsia*. 1998;39(12):1302–8.
19. Wang ZI, Jin K, Kakisaka Y, Mosher JC, Bingaman WE, Kotagal P, et al. Imag(in)ing seizure propagation: MEG-guided interpretation of epileptic activity from a deep source. *Hum Brain Mapp*. 2012;33(12):2797–801.
20. Shamji MF, Fric-Shamji EC, Benoit BG. Brain tumors and epilepsy: pathophysiology of peritumoral changes. *Neurosurg Rev*. 2009;32(3):275–85.
21. Perucca P, Dubeau F, Gotman J. Intracranial electroencephalographic seizure-onset patterns: effect of underlying pathology. *Brain*. 2014;137(1):183–96.
22. Englot DJ, Chang EF, Vecht CJ. Epilepsy and brain tumors. *Handb Clin Neurol*. 2016;134:267–85.
23. Mittal S, Barkmeier D, Hua J, Pai DS, Fuerst D, Basha M, et al. Intracranial EEG analysis in tumor-related epilepsy: evidence of distant epileptic abnormalities. *Clin Neurophysiol*. 2016;127(1):238–44.
24. Ghosh SS, Kakunoori S, Augustinack J, Nieto-Castanon A, Kovelman I, Gaab N, et al. Evaluating the validity of volume-based and surface-based brain image registration for developmental cognitive neuroscience studies in children 4 to 11 years of age. *Neuroimage*. 2010;53(1):85–93.
25. Kuroda N, Sonoda M, Miyakoshi M, Nariai H, Jeong JW, Motoi H, et al. Objective interictal electrophysiology biomarkers optimize prediction of epilepsy surgery outcome. *Brain Commun*. 2021;3(2):fcab042.
26. Wieser HG, Blume WT, Fish D, Goldensohn E, Hufnagel A, King D, et al. ILAE Commission Report. Proposal for a new classification of outcome with respect to epileptic seizures following epilepsy surgery. *Epilepsia*. 2001;42(2):282–6.
27. Nakai Y, Jeong JW, Brown EC, Rothermel R, Kojima K, Kambara T, et al. Three- and four-dimensional mapping of speech and language in patients with epilepsy. *Brain*. 2017;140(5):1351–70.
28. Stolk A, Griffin S, van der Meij R, Dewar C, Saez I, Lin JJ, et al. Integrated analysis of anatomical and electrophysiological human intracranial data. *Nat Protoc*. 2018;13(7):1699–723.
29. Kambara T, Sood S, Alqatan Z, Klingert C, Ratnam D, Hayakawa A, et al. Presurgical language mapping using event-related high-gamma activity: the Detroit procedure. *Clin Neurophysiol*. 2018;129(1):145–54.
30. Asano E, Muzik O, Shah A, Juhász C, Chugani DC, Sood S, et al. Quantitative interictal subdural EEG analyses in children with neocortical epilepsy. *Epilepsia*. 2003;44(3):425–34.
31. Frauscher B, von Ellenrieder N, Ferrari-Marinho T, Avoli M, Dubeau F, Gotman J. Facilitation of epileptic activity during sleep is mediated by high amplitude slow waves. *Brain*. 2015;138(6):1629–41.
32. Miyakoshi M, Kanayama N, Iidaka T, Ohira H. EEG evidence of face-specific visual self-representation. *Neuroimage*. 2010;50(4):1666–75.
33. Maris E, Oostenveld R. Nonparametric statistical testing of EEG- and MEG-data. *J Neurosci Methods*. 2007;164(1):177–90.
34. Trebaul L, Deman P, Tuyisenge V, Jedynak M, Hugues E, Rudrauf D, et al. Probabilistic functional tractography of the human cortex revisited. *Neuroimage*. 2018;181:414–29.
35. Sonoda M, Silverstein BH, Jeong JW, Sugiura A, Nakai Y, Mitsuhashi T, et al. Six-dimensional dynamic tractography atlas of language connectivity in the developing brain. *Brain*. 2021; in press. doi:10.1093/brain/awab225.
36. Yeh FC, Panesar S, Fernandes D, Meola A, Yoshino M, Fernandez-Miranda JC, et al. Population-averaged atlas of the macroscale human structural connectome and its network topology. *Neuroimage*. 2018;178:57–68.
37. Sugiura A, Silverstein BH, Jeong JW, Nakai Y, Sonoda M, Motoi H, et al. Four-dimensional map of direct effective connectivity from posterior visual areas. *Neuroimage*. 2020;210:116548.
38. Lavenex P, Amaral DG. Hippocampal-neocortical interaction: a hierarchy of associativity. *Hippocampus*. 2000;10(4):420–30.
39. Barth DS, Sutherling W, Engle J, Beatty J. Neuromagnetic evidence of spatially distributed sources underlying epileptiform spikes in the human brain. *Science*. 1984;223(4633):293–6.
40. Tanaka N, Peters JM, Prohl AK, Takaya S, Madsen JR, Bourgeois BF, et al. Clinical value of magnetoencephalographic spike propagation represented by spatiotemporal source analysis: correlation with surgical outcome. *Epilepsy Res*. 2014;108(2):280–8.
41. Bourdillon P, Ferrand-Sorbet S, Apra C, Chipaux M, Raffo E, Rosenberg S, et al. Surgical treatment of hypothalamic hamartomas. *Neurosurg Rev*. 2021;44(2):753–62.
42. Sugano H, Nakanishi H, Nakajima M, Higo T, Iimura Y, Tanaka K, et al. Posterior quadrant disconnection surgery for Sturge-Weber syndrome. *Epilepsia*. 2014;55(5):683–9.
43. Hamer HM, Najm I, Mohamed A, Wyllie E. Interictal epileptiform discharges in temporal lobe epilepsy due to hippocampal sclerosis versus medial temporal lobe tumors. *Epilepsia*. 1999;40(9):1261–8.
44. Shigeto H, Morioka T, Hisada K, Nishio S, Ishibashi H, Kira D, et al. Feasibility and limitations of magnetoencephalographic detection of epileptic discharges: simultaneous recording of magnetic fields and electrocorticography. *Neurol Res*. 2002;24(6):531–6.
45. Rikir E, Koessler L, Ramantani G, Maillard LG. Added value and limitations of electrical source localization. *Epilepsia*. 2017;58(1):174–5.
46. Wieser HG, Ortega M, Friedman A, Yonekawa Y. Long-term seizure outcomes following amygdalohippocampectomy. *J Neurosurg*. 2003;98(4):751–63.

47. Wieser HG. ILAE Commission Report. Mesial temporal lobe epilepsy with hippocampal sclerosis. *Epilepsia*. 2004;45(6):695–714.
48. Gross DW. Diffusion tensor imaging in temporal lobe epilepsy. *Epilepsia*. 2011;52(4):32–4.
49. Kodiweera C, Alexander AL, Harezlak J, McAllister TW, Wu YC. Age effects and sex differences in human brain white matter of young to middle-aged adults: a DTI, NODDI, and q-space study. *Neuroimage*. 2016;128:180–92.
50. Alarcon G, Garcia Seoane JJ, Binnie CD, Martin Miguel MC, Juler J, Polkey CE, et al. Origin and propagation of interictal discharges in the acute electrocorticogram. Implications for pathophysiology and surgical treatment of temporal lobe epilepsy. *Brain*. 1997;120(12):2259–82.
51. Taschenberger H, von Gersdorff H. Fine-tuning an auditory synapse for speed and fidelity: developmental changes in pre-synaptic waveform, EPSC kinetics, and synaptic plasticity. *J Neurosci*. 2000;20(24):9162.
52. Feldmeyer D, Lübke J, Sakmann B. Efficacy and connectivity of intracolumnar pairs of layer 2/3 pyramidal cells in the barrel cortex of juvenile rats. *J Physiol*. 2006;575(2):583–602.

SUPPORTING INFORMATION

Additional supporting information may be found online in the Supporting Information section.

How to cite this article: Mitsuhashi T, Sonoda M, Sakakura K, Jeong J-W, Luat AF, Sood S, et al. Dynamic tractography-based localization of spike sources and animation of spike propagations. *Epilepsia*. 2021;62:2372–2384. <https://doi.org/10.1111/epi.17025>